

Electroabsorption of polyacetylene

S. D. Phillips, R. Worland, G. Yu, T. Hagler, R. Freedman, Y. Cao,
V. Yoon, J. Chiang, W. C. Walker, and A. J. Heeger

*Department of Physics and Institute for Polymers and Organic Solids, University of California, Santa Barbara,
Santa Barbara, California 93106*

(Received 30 June 1989)

We present the results of electroabsorption measurements for nonoriented *cis*- and *trans*-polyacetylene and for oriented *trans*-polyacetylene. The electroabsorption spectrum of the as-grown (nonoriented) material is dominated by a series of field-induced absorptions and bleachings near the band edge. These spectral features are interpreted as vibronic sidebands (arising from electronic coupling to the excited-state phonon modes) which are broadened by the applied electric field. The existence of such vibronic sidebands in the as-grown material indicates that the band-edge states are localized. In oriented *trans*-(CH)_x the vibronic features (the strongest of which is observed as a "knee" near 1.5 eV in the absorption spectrum) are highly suppressed, while the induced absorption at 1.28 eV is enhanced relative to the unoriented case. No electroabsorption signal is present when the external field is applied perpendicular to the chain direction. The dependences of the electroabsorption spectrum on temperature, electric field strength, incident light polarization, and intensity are also presented. Since stretch orientation suppresses the vibronic sidebands, we conclude that such postsynthesis processing leads to improved structural order and to delocalization of the band-edge electronic states.

INTRODUCTION

Trans-polyacetylene [trans-(CH)_x] is the most thoroughly studied of all conducting polymers. As a result, there exists a wealth of experimental and theoretical results for this degenerate ground-state material. Optical excitations across the Peierls gap are believed to rapidly evolve to oppositely charged soliton pairs with associated localized states within the energy gap. Consequently, numerous experimental techniques have been employed to probe this range of excitation energies in an effort to gain information regarding these states.

A particularly rich area of the spectrum is near the absorption edge of *trans*-polyacetylene, located around 1.3–1.6 eV. At this energy several spectroscopic features have been reported including an infrared luminescence,¹ a photoinduced absorption feature,^{2–5} a shoulder or "knee" in the absorption spectrum,⁶ and the electric-field-induced absorption peaks.² In addition, it has been suggested^{7–9} that the direct photoproduction of solitons may occur near the energy. In this paper we focus on an experimental study of the electroabsorption features.

Franz¹⁰ and Keldysh¹¹ predicted in 1958 that the application of a uniform electric field should induce optical absorption below the energy gap of a semiconductor as a result of photon-assisted tunneling. These predictions were confirmed in electroabsorption^{12–14} and electroreflection^{15–17} experiments. Since these techniques provide a very sensitive probe of externally induced changes in the optical spectrum they have been used extensively to probe the band structures of inorganic semiconductors.^{18–20} Calculations by Aspnes and Rowe^{21,22} showed that the quantum-mechanical expressions for the electric-field-induced changes in the optical constants, in

the limit of large broadening, produced modulation spectra which were related to the third derivative of the unperturbed optical spectrum. This third derivative regime was found to occur only if the energy gained by an electron upon acceleration by the field was less than the broadening parameter.²³ At higher field strengths the full quantum-mechanical treatment of Franz and Keldysh is necessary, and at very high fields (not normally attained) the field drop across the unit cell is so large that the band structure itself is altered (the Stark effect). Reviews of electromodulation spectroscopy of localized excitations (e.g., *F* centers) have been presented by Luty²⁴ and Grassano.²⁵ Dow²⁶ has also reviewed the effects of modulation spectroscopy on excitons. Recently electroabsorption of quantum-well structures has been interpreted in terms of the quantum confined Stark effect as described by Miller *et al.*²⁷

Several researchers have performed electroabsorption experiments on molecular crystals such as tetracene, pentacene,²⁸ and anthracene,²⁹ and also on single crystals of the conjugated polymer polydiacetylene [PTS,³⁰ DCHD,³¹ and TCDU (Ref. 32)]. They found the polydiacetylene systems to be highly anisotropic with little or no signal when the field was applied perpendicular to the chain axis. The modulation spectra were related to first and second derivatives of the unperturbed absorption spectra and scaled quadratically with the applied field. Orenstein *et al.*² investigated electroabsorption spectra in nonoriented polyacetylene and found it to be related to the second derivative of the unperturbed absorption coefficient. The relationship between photoinduced absorption features and the electroabsorption spectrum has been investigated by several researchers.^{2,3,33} Initial results on the anisotropy of the electroabsorption signal as

a function of angle between the optical polarization and the field direction were presented by Worland *et al.*³⁴ for nonoriented *trans*(CH)_x and poly(3-hexylthiophene).

In considering the optical properties of a sample, the transmitted intensity I_T may be written in terms of the sample thickness d , absorption coefficient α , and reflection coefficient R as

$$I_T = I_0(1-R)^2 e^{-\alpha d}, \quad (1)$$

where we have assumed the same reflection coefficient from the front and back surfaces of the sample and neglected multiple reflections. The effect of the modulation field, F , can be expressed as

$$\frac{\partial I_T}{\partial F} = -I_0 e^{-\alpha d} \left[d(1-R)^2 \frac{\partial \alpha}{\partial F} + 2(1-R) \frac{\partial R}{\partial F} \right]. \quad (2)$$

Dividing by the unperturbed intensity yields

$$\frac{-\Delta I_T}{I_T} = \frac{-\Delta T}{T} = d\Delta\alpha + \frac{2}{1-R} \Delta R, \quad (3)$$

where T is the transmission coefficient. Writing this in terms of the complex index of refraction, $N = n + ik$, where $k = \alpha c / 2\omega$ and using the relation

$$R = \frac{(n-1)^2 + k^2}{(n+1)^2 + k^2} \quad (4)$$

for normal incidence yields

$$\frac{-\Delta T}{T} = \left[2(n\Delta n + k\Delta k) - \left(\frac{k^2+1}{n} \right) \Delta n \right] + \frac{4\pi d}{\lambda} \Delta k. \quad (5)$$

For polyacetylene,^{35,36} n and k are such that the last term of Eq. (5) is typically more than an order of magnitude larger than the first term for film thickness $\geq 0.2 \mu\text{m}$; thus $\Delta T/T \approx -\Delta\alpha d$. If the thickness of the sample is known, we can, therefore, obtain from the electroabsorption spectrum the values of $\Delta\alpha$ (and hence Δk) as a function of wavelength. Though Kramers-Kronig analysis, the changes in the real part of the index of refraction, Δn , can then be calculated.

EXPERIMENT

The apparatus used to investigate the electroabsorption spectrum consisted of a grating monochromator with a tungsten-halogen light source and appropriate filters to prevent second-order light from reaching the sample. The optical resolution at the exit slits was typically 50 \AA and the data point increment was 10 \AA . For experiments involving polarized light, a near-infrared polarizer was used to establish the polarization and a half-wave plate (optimized at 850 nm) was used to rotate the polarization vector of the light. The sample was mounted on a one-inch-diam sapphire disk (zero orientation) on which 100 \AA of chromium (for surface adhesion) and 1000 \AA of gold were successively deposited in the form of two semicircular pads with a 0.5-mm gap located between them. The semitransparent polymer sample was located across this gap.

Thin ($\approx 0.2 \mu\text{m}$) films of nonoriented polyacetylene were grown directly on the substrate using either the standard Shirakawa³⁷ method or the modified catalyst developed by Akagi *et al.*³⁸ The *cis*-(CH)_x samples were loaded into a liquid-nitrogen cold finger as soon as possible; however, they still contained approximately 20% *trans* content due to partial conversion during the synthesis and handling procedure.³³ The *trans*-(CH)_x samples were isomerized for 50 min at 170°C under high vacuum. Conductivities of the films, as inferred from resistance measurements ($R \approx 10^9 \Omega$), were typically $\sim 10^{-5} \text{ S/cm}$.

Free-standing films used to make the oriented samples were synthesized using the catalyst developed by Akagi *et al.* since the results in a somewhat more stretchable film than the standard synthesis. The films were mechanically stretched by a factor of 4–6 in an argon dry box and then isomerized as outlined above. No attempt was made to examine stretched *cis*-(CH)_x films since the prolonged mechanical handling would result in a large *trans*-(CH)_x content. As a check of sample quality, some stretched samples were doped with iodine yielding a conductivity of $20\,000 \text{ S/cm}$ (these doped samples were not used in the electroabsorption experiment). The thickness of the nonoriented free-standing films was $\approx 4.5 \mu\text{m}$ and that of the stretched ($5\times$) films was $\approx 3 \mu\text{m}$ as measured by a comparative indicator with a resolution of $\pm 0.1 \mu\text{m}$. The free-standing polymer films were again evaporated with gold (no chromium) electrodes onto their upper surface and attached with silver paint to the substrate electrodes, thus ensuring that the electric field developed across the gap was uniform throughout the thick sample. For thin films grown directly onto the substrate, the substrate electrodes were sufficient to provide a uniform field. This was checked by measuring the electroabsorption with both substrate only and substrate plus surface electrodes present and observing no change in the spectrum.

The high voltage supply consisted of a sinusoidal audio oscillator connected to a power amplifier and then to a 20:1 high voltage transformer. The voltage was monitored at the output of the transformer with a high voltage oscilloscope probe (Tektronix P6015) which provided both the voltage measurement (via a digital oscilloscope), and a convenient reference signal for the lock-in amplifier. This arrangement was capable of generating voltages of 2000 V peak amplitude, hence peak fields of 40 kV/cm over a frequency range of $200\text{--}9000 \text{ Hz}$. The high voltage was applied to the sample via stainless steel feed-through leads into the cryostat to the sample holder. Contact to the gold electrode pads was achieved by spring loaded (Pt/Ir) pins. The cryostat was evacuated to a pressure of $\approx 10^{-5} \text{ torr}$, and the sample temperature was controlled either by a cold finger for liquid-nitrogen temperature, or with a helium gas flow cooling head for continuous temperature variation down to 20 K . Light transmitted through the semitransparent sample was detected by a silicon photodiode and the output was sent to a lock-in amplifier and simultaneously to an analog-to-digital (A-D) converter. The use of the lock-in allowed detection (both in magnitude and phase) of small changes

in the transmitted intensity due to the application of the electric field, while the A-D converter concurrently recorded the total transmitted intensity.

The electric field produced during the positive portion of the voltage biasing cycle has the same effect as that of the negative portion on the centrosymmetric polymer system. This was verified by the absence of any electroabsorption signal at the fundamental frequency. Since the voltage source was sinusoidal ($\sin \omega t$) and the response is quadratic in the applied field, the instantaneous change in the transmission coefficient for an induced bleach (i.e., $\Delta T=0$) is proportional to $F_0^2 \sin^2(\omega t) = \frac{1}{2} F_0^2 [1 - \cos(2\omega t)]$. The lock-in amplifier reference was set to twice the fundamental $\sin 2\omega t$, hence the dynamical component of the electroabsorption signal $[-\cos(2\omega t) = \sin(2\omega t - \pi/4)]$ had a phase of $-\pi/4$ relative to the lock-in reference. Similarly, an induced absorption had a phase of $+\pi/4$ relative to the reference. The measured phase of the electroabsorption signals agreed well with these values, and the transition from an absorption to a bleach corresponded to an abrupt 180° phase change of the signal. The output of the lock-in, which is the rms signal strength, was multiplied by $2^{3/2}$ so that we report the peak value of $\Delta T/T$ induced for a given peak field strength.

All components of the apparatus were checked for their frequency response. The high voltage scope probe, which is specified to be linear over a frequency range of several megahertz, was checked against a probe known to be linear over this range and found to be in good agreement. The photodiode response was checked by using an infrared LED driven by a square wave generator (with a small resistive load placed in series to limit the current) at a constant voltage, as the frequency of the generator was varied. The photodiode output was in phase with the LED and of nearly constant magnitude over the entire frequency range of interest (decreasing by 10% at 20 000 Hz). The total stray capacitance of the high voltage cables, stainless steel feedthroughs, and sample configuration was negligible ($< 10^{-13}$ F as measured with an LCR meter). Electromagnetic pickup from the high voltage source was not detectable, as checked by blocking the exit slits of the monochromator and observing no detectable signal at the lock-in amplifier. The optical intensity dependence of the electroabsorption signal was obtained using a series of calibrated neutral density filters. Unperturbed absorption curves were obtained by dividing the transmitted intensity by a reference scan (using a blank substrate).

RESULTS

Figure 1 displays the absorption and electroabsorption spectra at 80 K and 25 kV/cm field strength (using unpolarized light), of a thin ($\approx 0.2 \mu\text{m}$), unoriented film of *trans*-(CH)_x grown directly on the substrate by the Akagi synthesis. The electroabsorption spectrum is similar to that produced by the conventional Shirakawa^{2,34} method although the low-energy (1.28 eV peak is noticeably more pronounced (see Fig. 3). The spectrum consists of a series of field-induced absorption maxima (1.28, 1.42, 1.53, 1.64,

1.75 eV) and minima (1.33, 1.48, 1.59, 1.69, 1.79 eV). The electroabsorption spectrum as a whole shifts to lower energy with decreasing temperature (by 0.040 eV at 80 K relative to 300 K); this is due to a decrease in the band gap since the electroabsorption peaks remain fixed with respect to each other and to the band edge. The electroabsorption features become slightly sharper and increase in magnitude (by $\approx 25\%$) upon cooling from room temperature to liquid-nitrogen temperature, with little further change at lower temperatures. The dependence of the electroabsorption spectrum at all wavelengths is quadratic in applied field strength ($F^{2.0 \pm 0.1}$).

To check for Joule heating effects, which would also induce optical perturbations at 2ω , we investigated the dependence of the electroabsorption spectrum on the frequency of the applied field, at a constant field strength. The electroabsorption signal increased roughly linearly with increasing frequency, by 50% over the frequency range accessible with our equipment ($2f = 400\text{--}18\,000$ Hz). The modest increase is in contrast to that expected from thermally generated changes in transmission which would decrease with increasing frequency. As described in the experimental section, we extensively checked our apparatus for frequency-dependent components and found none, so we interpret the observed increase as a real effect, probably due to dielectric relaxation.³⁹ The dependence of the electroabsorption signal upon incident optical intensity is linear (1.0 ± 0.05), as is the transmitted intensity; hence $\Delta T/T$ is intensity independent.

Figure 2 displays the anisotropy in electroabsorption signal of unoriented *trans*-(CH)_x (80 K, 25 kV/cm) at 1.42 eV, as a function of angle between the incident optical polarization and the field direction. Although the sample is not oriented, this technique can be used to infer the anisotropy of the signal with respect to the direction of the polymer chains.⁴⁰ The observed anisotropy ($I_{\text{max}}/I_{\text{min}}$) is 2.3 ± 0.1 , with the maximum signal occurring when the polarization of the light is along the field direction. We have scanned the entire electroabsorption spectrum with the optical polarization both perpendicular and parallel to the applied field and found that the an-

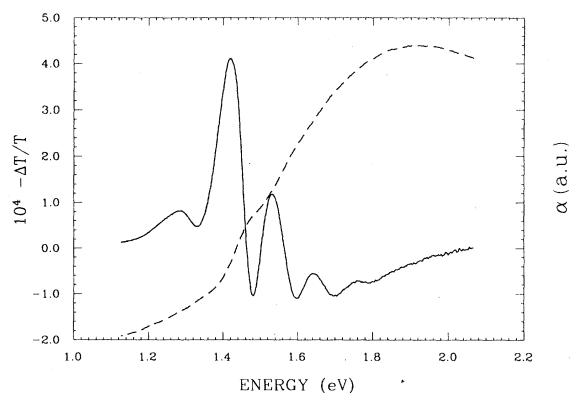


FIG. 1. The absorption coefficient (dashed line) and the electroabsorption (solid line) spectrum (80 K, 25 kV/cm) of a thin film of unoriented *trans*-polyacetylene.

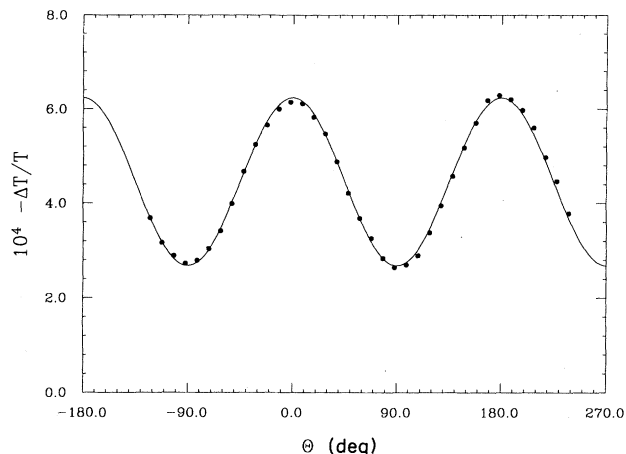


FIG. 2. The anisotropy in electroabsorption signal of unoriented *trans*-polyacetylene (80 K, 25 kV/cm) as a function of angle between the incident optical polarization and the field direction.

isotropy of 2.3 holds for all electroabsorption features.

Figure 3 illustrates the relationship between a typical electroabsorption spectrum (from the standard Shirakawa synthesis) and the second derivative of the unperturbed absorption coefficient with respect to photon energy. The modulation spectrum clearly reveals salient features present in the unperturbed absorption spectrum. The oscillations above 1.35 eV fit well to the second derivative of the unperturbed absorption curve. We have examined eight separate samples and found similar results. However, the small feature at 1.28 eV is not accounted for in the second derivative spectra.

The absorption coefficient and electroabsorption spectrum for *cis*-(CH)_x (80 K, 25 kV/cm) are shown in Fig. 4. The electroabsorption peaks are located at 2.02, 2.19, and

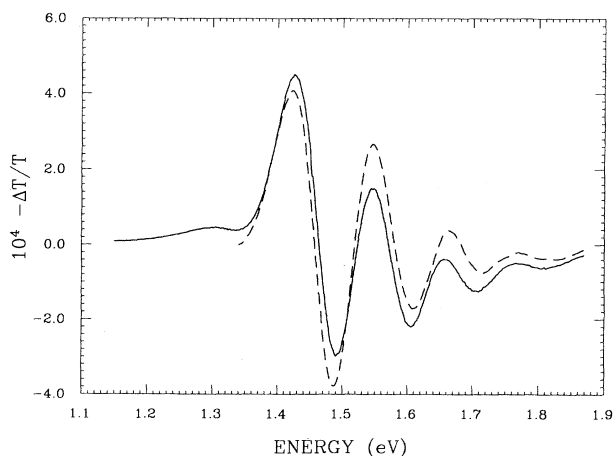


FIG. 3. The relationship between a typical electroabsorption spectrum of *trans*-polyacetylene and the second derivative of the unperturbed absorption coefficient with respect to photon energy.

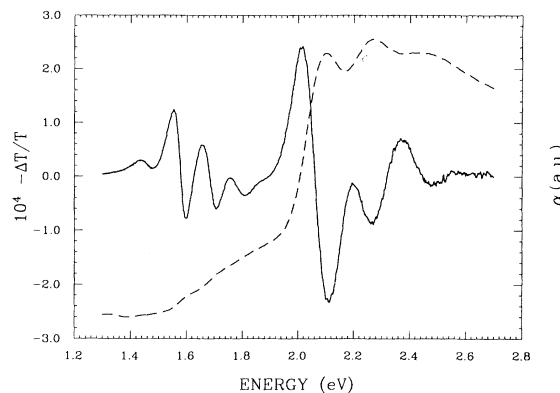


FIG. 4. The absorption coefficient (dashed line) and the electroabsorption spectrum (solid line) for *cis*-polyacetylene (80 K, 25 kV/cm).

2.37 eV while the minima are at 2.11, 2.26, and 2.47 eV. Below 1.8 eV the existence of a fraction of the *trans* isomer is clearly evident, although blue shifted by 0.12 eV, perhaps due to confinement between adjacent *cis* regions. The *cis*-(CH)_x electroabsorption spectrum also closely corresponds to the spectrum derivative of the corresponding unperturbed absorption spectrum, but there is a slight energy shift (0.02 eV) between the two.

The electroabsorption spectra of free-standing films of *trans*-(CH)_x are presented in Fig. 5. The dashed line represents the unoriented free-standing film electroabsorption spectrum which has been scaled to account for the difference in sample thickness (by a factor of 3.0/4.5 μm or 0.66). The lack of any orientation of this sample was directly verified by measuring a constant transmitted intensity for all incident optical polarizations. The electroabsorption spectrum of a stretch-oriented (5×) sam-

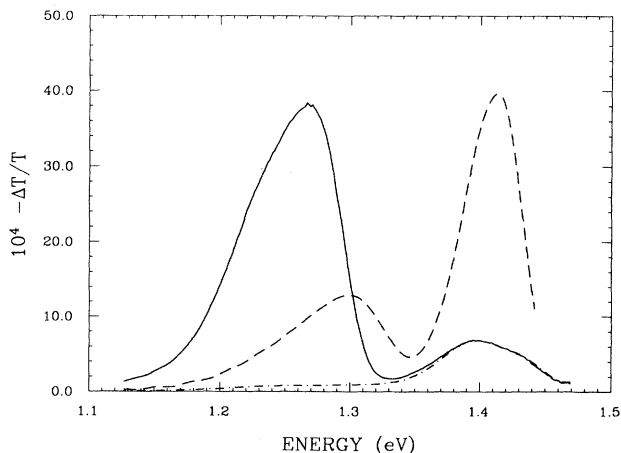


FIG. 5. The electroabsorption spectra of *trans*-polyacetylene; an unoriented free-standing film (dashed curve), a stretch-oriented (5×) free-standing film with the chain direction parallel to the field direction and the optical polarization parallel (solid curve) and perpendicular (dot-dashed curve) to the field.

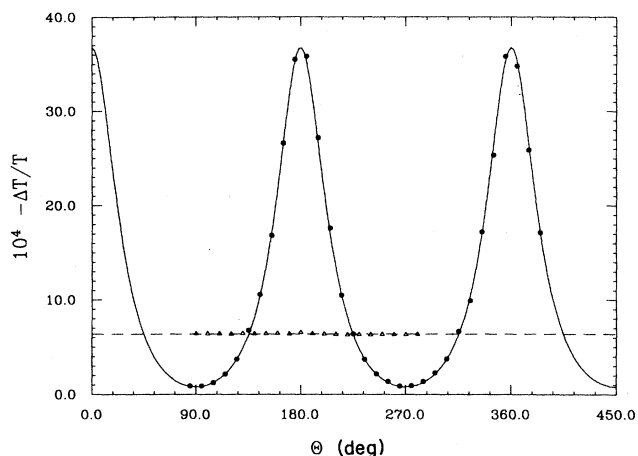


FIG. 6. The anisotropy of the electroabsorption features of the oriented sample; solid circles are the 1.27-eV peak; open triangles are the 1.42-eV feature.

ple with both the chain direction and the optical polarization parallel to the field direction is given by the solid curve. This spectrum is limited to the near-infrared region since the thick films are completely opaque in the visible. The 1.42-eV feature (one of the several vibronic sidebands) is strongly suppressed relative to the low-energy peak and to that found in the unoriented material. The low-energy (1.27 eV) absorption is slightly red shifted and substantially enhanced relative to the corresponding feature in the unoriented electroabsorption spectrum taken with unpolarized light. It should be noted that the low-energy feature is related to the first derivative of the unperturbed absorption spectrum while the suppressed 1.42-eV peak continues to have a second derivative line shape. The dot-dashed curve is the spectrum with the chain direction parallel to the field, but with the optical polarization perpendicular to it and shows very little electroabsorption signal at any wavelength.

Since the thick films are completely opaque in the visible, we were able to check for pin holes; none were found. Spectra on samples stretched 4–6 \times showed similar electroabsorption features and anisotropy. The electroabsorption spectrum with the chains mounted perpendicular to the field direction was considerably noisier and produced no detectable signal ($\Delta T/T < 10^{-5}$). Some of the stretch-oriented samples were compensated with anhydrous ammonia gas (20 torr for 3 h) to check that the electroabsorption spectrum was not a result of impurities which are known to have optical absorptions in this region.⁴¹ The compensated samples showed the same electroabsorption spectrum (with slightly broadened features) and anisotropy as the uncompensated samples, thus ensuring that the electroabsorption effects are not the result of extrinsic impurities.

The anisotropy of the electroabsorption features of the oriented samples is shown in Fig. 6. The suppressed 1.42-eV electroabsorption feature is clearly isotropic with respect to incident optical polarization and fits very well to a constant of $-\Delta T/T = 6.4 \times 10^{-4}$. In contrast, the

low-energy feature centered at 1.27 eV is strongly anisotropic with a maximum when the polarization direction coincides with the chain axis (and the field direction).

Figure 7 displays the result of a Kramers-Kronig analysis (based on the data in Fig. 3) by which Δn is calculated (from Δk) and combined with the linear optical constants^{35,42} to compute the third-order nonlinear susceptibility $\chi_{dc}^{(3)}(\omega, 0, 0)$ involved in the electroabsorption process from

$$\chi_{dc}^{(3)}(\omega, 0, 0) = \frac{N\Delta N}{2\pi F^2} = \frac{\Delta\epsilon}{4\pi F^2}. \quad (6)$$

Hence the real and imaginary parts of $\chi^{(3)}$ are related to field-induced changes in the dielectric function (ϵ).

We note that the field-induced change in the real part of the index of refraction (Δn) at 1.17 eV (1.06 μm) for stretch-oriented *trans*-polyacetylene (i.e., the solid curve in Fig. 5) is 1.8×10^{-5} at a field strength of 25 kV/cm, as shown in Fig. 8. Since the magnitude goes as F^2 , one can extrapolate to a value of Δn (1.17 eV) $\approx 8 \times 10^{-3}$ at a field of 5×10^5 V/cm. Using published numbers⁴³ for LiNbO₃ (electro-optical coefficient $r = 30.8$ pm/V), we estimate a value for Δn from the linear electro-optic effect of the same magnitude. Thus, because of their large third-order susceptibilities, it may be possible to utilize conjugated polymers with a center of symmetry in electro-optical devices.

DISCUSSION

To analyze the spectra of the polyacetylene films we define a coordinate system with the direction of light propagation in the $+z$ direction, the polymer sample located in the x - y plane with thickness d , and the electric field direction along the x axis. Let a polymer chain make an angle ϕ with the x axis and the optical polarization vector an angle Θ with the x axis. We define a subscript notation where \parallel (\perp) denotes the direction parallel (perpendicular) to the polymer chain. Thus the transmission coefficient for a polymer chain is given by

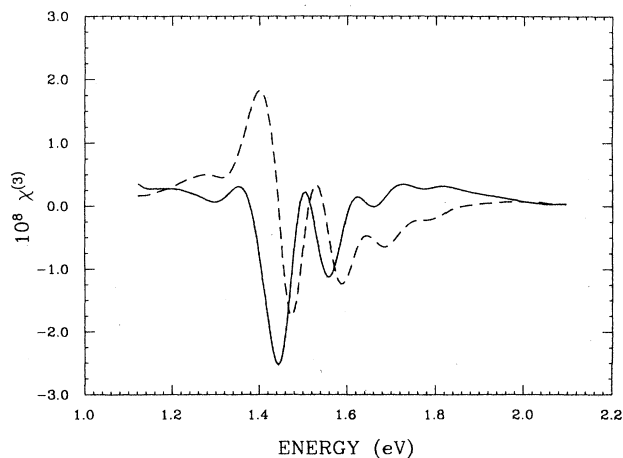


FIG. 7. The real (solid curve) and imaginary (dashed curve) parts of $\chi_{dc}^{(3)}(\omega, 0, 0)$.

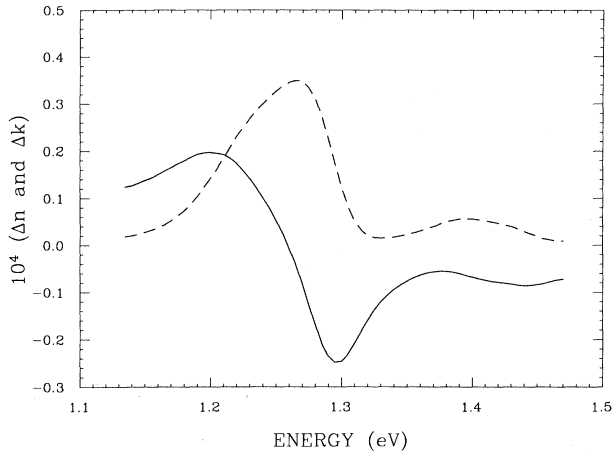


FIG. 8. The real (solid curve) and imaginary (dashed curve) parts of the complex index of reflection for oriented *trans*-polyacetylene (80 K, 25 kV/cm) with both the field and optical polarization parallel to the chain direction.

$$T(\Theta - \phi) = (1 - R_{\parallel})^2 e^{-\alpha_{\parallel} d} \cos^2(\Theta - \phi) + (1 - R_{\perp})^2 e^{-\alpha_{\perp} d} \sin^2(\Theta - \phi). \quad (7a)$$

The application of the modulation field perturbs the absorption coefficient α_i ($i = \parallel, \perp$) by $\Delta\alpha_i$ where $\Delta\alpha_i$ is proportional to F^2 . Since $\alpha_i d < 10$ in the spectral region considered and $\Delta\alpha_i < \alpha_i$, $\Delta\alpha_i d \ll 1$, and

$$e^{-\alpha_i(F)d} \approx e^{\alpha_i d} (1 - \Delta\alpha_i d). \quad (7b)$$

The change in transmission coefficient due to the field can be expressed as

$$-\Delta T = d [T_{\parallel} \Delta\alpha_{\parallel} \cos^2(\Theta - \phi) + T_{\perp} \Delta\alpha_{\perp} \sin^2(\Theta - \phi)], \quad (8)$$

where

$$T_i = (1 - R_i)^2 e^{-\alpha_i d}.$$

(i) *Oriented case.* For the case with the polymer oriented along the field direction ($\phi = 0$)

$$\frac{-\Delta T}{T} = \frac{d [T_{\parallel} \Delta\alpha_{\parallel} \cos^2(\Theta) + T_{\perp} \Delta\alpha_{\perp} \sin^2(\Theta)]}{T_{\parallel} \cos^2(\Theta) + T_{\perp} \sin^2(\Theta)}. \quad (9)$$

Equation (9) provided the fitting function used in Fig. 6, where the ratio of transmission coefficients (T_{\perp}/T_{\parallel}) was set to the experimentally observed value (5.54 at 1.27 eV, 17.9 at 1.42 eV). The electroabsorption feature at 1.27 eV is highly anisotropic (see Fig. 6) and is slightly red shifted with respect to that observed in the unoriented films. The data are accurately described by Eq. (9), yielding a value of $\Delta\alpha_{\parallel}/\Delta\alpha_{\perp} = 44$. In contrast, the 1.42-eV feature is strongly suppressed relative to its magnitude in the unoriented material (Fig. 5). Furthermore, $\Delta T/T$ is isotropic in polarization angle as clearly seen in Fig. 6. The residual signal is not simply due to some remaining unoriented (but crystalline) fraction of the polymer since

that would be expected to show an anisotropy similar to that of Fig. 2. The isotropic feature implies that there exists a small (5%) fraction of residual amorphous material in the oriented polymer. Consequently, it may be that the 1.27-eV electroabsorption feature is strictly one dimensional and that $\Delta\alpha_{\perp}$ (1.27 eV) is largely due to this residual fraction of amorphous material.

(ii) *Unoriented case.* The transmission coefficient for an unoriented sample can be written

$$T = \left[1 - \frac{R_{\parallel} + R_{\perp}}{2} \right]^2 e^{[-(\alpha_{\parallel} + \alpha_{\perp})/2]d}. \quad (10)$$

The unoriented polymer has, in general, the chain direction at an arbitrary angle with respect to the field. From the results on the oriented material, we know that there is negligible signal when the field is applied perpendicular to the chains, so we will only consider terms involving the field projected onto the chain axis. The random chain direction can be accounted for by integrating over all possible chain angles, resulting in a change in the fractional transmission coefficient given by

$$\frac{-\Delta T}{T} = \frac{d}{8} \{ \Delta\alpha_{\parallel} [2 \cos^2(\theta) + 1] + \Delta\alpha_{\perp} [-2 \cos^2(\theta) + 3] \}, \quad (11)$$

where θ is the angle between the optical polarization vector and the applied field.

The anisotropy of the nonoriented samples is consistently found to be a maximum at $\theta = 0 \pm 5^\circ$ (see Fig. 2); thus the second term in Eq. (11) containing the factor $\Delta\alpha_{\perp}$ must be negligible. This is consistent with the data from the 1.27-eV feature of the oriented material where $\Delta\alpha_{\parallel} = 44\Delta\alpha_{\perp}$. Using these values from the oriented sample predicts an anisotropy in the unoriented material of

$$\frac{-\Delta T(0^\circ)}{-\Delta T(90^\circ)} = \frac{3\Delta\alpha_{\parallel} + \Delta\alpha_{\perp}}{\Delta\alpha_{\parallel} + 3\Delta\alpha_{\perp}} = 2.83. \quad (12)$$

This value is somewhat larger than the observed anisotropy of 2.3 in the nonoriented samples, hence the chains of the oriented material are more nearly one dimensional than the as-grown nonoriented material, perhaps due to an increase in the mean conjugation length upon stretching. Equation (11) is of the form $A(1 + B \cos^2\theta)$ which was used for the fitting function of Fig. 2; the best fit yielded $B = 1.3$, implying $\Delta\alpha_{\parallel} = 8.4\Delta\alpha_{\perp}$ for the polymer chains in the nonoriented material.

To compare the electroabsorption of the nonoriented material directly to that of a sample of the same thickness with both the optical polarization and chain orientation in the field direction we need to consider the ratio of the angular average of Eq. (11) to Eq. (9) evaluated at $\theta = 0$. Considering only the $\Delta\alpha_{\perp}$ term of Eq. (11) we find

$$\frac{-\Delta T/T|_{\text{unoriented}}^{(\Theta)}}{-\Delta T/T|_{\text{oriented}}^{\Theta=0}} = \frac{1}{4}. \quad (13)$$

It is important to note that Eq. (13) assumes that $\Delta\alpha_{\parallel}$ is the same for both the nonoriented and oriented materials. Equation (13) implies that in stretching the polymer it is only necessary to consider the geometrical projections of

the field and the optical polarization, onto the chain axis. By scaling the nonoriented absorption curve shown in Fig. 5 by a factor of 4, we see that this assumption appears to be approximately correct for the low-energy electroabsorption feature at 1.27 eV where the predicted and measured electroabsorption signals (for polarized light and an oriented sample) are in reasonable agreement to within about 30%. The assumption completely fails for the 1.42-eV electroabsorption peak where the predicted and measured signals differ by a factor of 25.

(iii) *Interpretation.* In considering the origin of the electroabsorption spectral features of polyacetylene, it is useful to examine data which do not include electric field modulation. We concentrate first on those features of the electroabsorption spectrum above 1.35 eV which are associated with second derivative of the unperturbed absorption coefficient. As shown through thermal modulation spectra,³³ reflectance data,⁴⁴ and the second derivative of the unperturbed absorption coefficient (see Fig. 3), there exists, in the absence of any applied field, a series of vibrational peaks located at the same position and energy spacing as those found in the electroabsorption spectrum. It is important to keep in mind while examining the various spectra that the vibrational sideband appears as a secondary peak (or a "knee") in an absorption spectrum, as a zero crossing in a thermal modulation (first derivative) spectrum, and as an absorption minimum (bleaching maximum) in a second derivative electroabsorption modulation spectrum. It should also be noted that the 80-K spectra are red shifted by 0.04 eV relative to the room-temperature spectra.

A general expression for the absorption spectrum, including vibronic sidebands, can be written as follows:

$$\alpha(\epsilon) = \sum_{\{v\}} \alpha^0 \left[\epsilon - \sum_v v \hbar \omega_0 \right] e^{-S(S^v/v!)} , \quad (14)$$

where the sum $\{v\}$ is on all possible excited vibrational states of the optical phonon with energy $\hbar \omega_0$, ϵ is the photon energy, $\alpha^0(\epsilon)$ is the absorption coefficient in the absence of vibronic effects, and S is the Huang-Rhys factor [in Eq. (14), we have assumed coupling to a single optical phonon]. The Huang-Rhys factor⁴⁵ is a measure of displacements in the configurational coordinate of the excited state relative to the ground state; i.e., S measures the change in the energy of the lattice due to an excitation on one electron from the ground state to the first excited state. Since in an ordered semiconductor, the band wave functions are extended over the entire lattice, the change in charge distribution (which leads to a change in the configurational coordinate) due to the photoexcitation is negligible; thus S should be of order $1/N$. Consequently, in conventional semiconductors with delocalized electronic levels, such vibronic features are neither expected nor observed.

Vibronic transitions involving optical phonons in the absorption between the localized levels in small molecules are, however, well known. Thus the existence of the vibronic features implies that the band-edge wave functions in polyacetylene are localized. This is consistent with the

fact that quasi-one-dimensional systems are especially sensitive to localization by disorder.⁴⁶ It has been suggested by Moses *et al.*⁴⁵ that the combination of a small amount of localization (i.e., a finite Huang-Rhys factor) and a sharp feature in the density of states, such as the divergence at the band edge of a one-dimensional semiconductor, leads to the appearance of vibronic structure in the absorption spectrum. Their analysis assumes a constant localization length (as a function of energy) for all states and leads to a series of progressively smaller vibrational peaks appearing above the absorption maximum.

In general, however, the localization length (l) is a strong function of the energy, $l(\epsilon)$ being maximum for states near (or below) the three-dimensional band edge; i.e., the usual situation for disorder-induced band tails. Thus we expect the Huang-Rhys factor to be a maximum near the band edge and to fall off in magnitude for transition energies involving initial and final states well into the band. Indeed, as seen in Fig. 1, the observed vibronic progression begins below the absorption peak. The existence of well-defined vibronic sideband structure implies that the product of the Huang-Rhys factor and the joint density of states is peaked at an energy below the absorption maximum, in the vicinity of the three-dimensional band gap. The observation that stretching the sample suppresses the vibrational modes, therefore, implies that chain orientation leads to a corresponding increase in the localization length for states with transition energies near the energy of the three-dimensional gap (and indirectly implies an improvement in structural order).

The phonon structure involved in the vibronic series is that of the electronic excited state of the polymer; i.e., after the interband transition, as given by Eq. (14) and the Franck-Condon principle. Consequently, the optical phonons ($\hbar \omega = 0.11$ eV from Fig. 1) involved in the process would be expected to be of lower energy than those found in the ground electronic state where the lowest optical phonon⁴⁷ has energy 0.132 eV. In a simple molecular-orbital picture of the excited state, an electron has been removed from a bonding orbital and placed in an antibonding orbital; hence this should soften the mode.

The evidence supports the assignment of the electroabsorption features above 1.35 eV as due to excited-state phonon vibronic sidebands associated with disorder-induced localized states near the band edge. The "knee" typically observed in the absorption spectrum at 1.5 eV is thus vibronic in origin, as initially suggested by Orenstein *et al.*² We emphasize, however, that through postsynthesis processing (stretch orientation) the disorder can be reduced to the point where the vibronic sidebands are heavily suppressed. The residual vibronic is isotropic, implying that it originates in a small residual fraction of amorphous material.

The interaction of the electric field with the localized band-edge electronic states leads to the second derivative relationship between the unperturbed absorption coefficient and the electroabsorption spectrum. As is well known, if a Gaussian peak is slightly broadened while conserving oscillator strength, the difference spectrum is

exactly the second derivative of the original Gaussian, within a scale factor. This implies that the electroabsorption spectrum is dominated by field-induced broadening.

The nature of the 1.27-eV feature is less clear. Although we do not have sufficient information to firmly assign the origin of this feature, we discuss some of the various possibilities.

(1) Although another phonon mode is possible, its persistence upon stretching makes this appear unlikely; any tendency toward localization (which would result in vibrational modes appearing in the energy gap) should be reduced by the improved structural order upon stretching and would be expected to affect all localized phonon modes similarly.

(2) Band-structure calculations⁴⁸ have predicted that the three-dimensional band gap may be located near 1.1 eV. The ability of electroabsorption measurements to locate such critical points in the joint density of electronic states is well known.¹⁸⁻²⁰ However, the strong anisotropy in favor of an intrachain absorption process (see Fig. 6) rules out the possibility that this feature is a result of interchain interactions.

(3) Although a bound exciton is possible, the fact that the photoconductivity onsets at about the same energy suggests that charged carriers are involved. In addition the anisotropy implies that such an exciton must be one dimensional as opposed to oppositely charged excitations on adjacent chains.

(4) It is possible that the 1.27-eV feature marks the onset of absorption enabled by the nonlinear quantum fluctuations of the lattice as suggested by Matsuoka and co-workers. Zero-point motion involving $S\bar{S}$ pairs is predicted to lead to a contribution to the optical absorption at energies $\hbar\omega$ such that $4\Delta/\pi < \hbar\omega < 2\Delta$ where 2Δ is the one-dimensional Peierls gap. Since the probability of an $S\bar{S}$ pair fluctuation with S and \bar{S} separated to infinity is negligible, the onset of absorption is at $\varepsilon = 4\Delta/\pi$ (i.e., the absorption is zero at threshold). However, weak interchain confinement due to adjacent chain phasing will shift the onset energy to somewhat greater than $4\Delta/\pi$ and lead to a finite absorption at threshold. Interaction

with the external field may modulate this onset energy leading to the observed first derivative line shape.

SUMMARY AND CONCLUSION

By carrying out electroabsorption measurements, we have investigated the effect of an external electric field on the absorption spectrum of *cis*- and *trans*-polyacetylene. A series of oscillations, which have been identified as vibronic sidebands, appear on the band edge of the absorption spectrum; these vibronic features are brought out clearly through electric field modulation. We have argued that these oscillations arise as sidebands to the interband transition from coupling to the optical phonon modes characteristic of the excited state and that their existence is due to localization of the electronic wave functions at energies near the band edge. Upon stretch orientation of the *trans* isomer, the vibronic modes are strongly suppressed, indicative of delocalization of the band-edge states through postsynthesis processing. In contrast, the low-energy ($\hbar\omega = 1.27$ eV) feature is enhanced by stretch orientation and is highly anisotropic with maximum when the light is polarized along the chain direction. This implies that the low-energy feature is intrinsic to the intrachain π -electronic structure. The onset of absorption at 1.27 eV is modulated by the external field via a second-order Stark effect. Since the one-dimensional band gap is at a higher energy, we conclude that the 1.27-eV threshold is either the signature of a one-dimensional exciton or the onset of the direct photoproduction of soliton-antisoliton pairs.

ACKNOWLEDGMENTS

The synthetic work and sample preparation were supported by the Office of Naval Research (N00014-83-K450); the electroabsorption measurements were supported by a contract from DARPA-AFOSR (ARPA order A.O. 6381/00; AFOSR Contract No. F49620-88-C-0138). Dr. S. Phillips was partially supported by the Army Research Office.

¹E. A. Imhoff, D. B. Fitchen, and R. E. Stahlbush, *Solid State Commun.* **44**, 329 (1982).

²J. Orenstein, G. L. Baker, and Z. Vardeny, *J. Phys. (Paris) Colloq.* **3**, C3-407 (1983).

³Z. Vardeny, E. Ehrenfreund, and O. Brafman, *Synth. Met.* **17**, 349 (1987).

⁴J. Orenstein and G. L. Baker, *Phys. Rev. Lett.* **49**, 1043 (1982).

⁵R. H. Friend, D. D. C. Bradley, and P. D. Townsend, *J. Phys. D* **20**, 1367 (1987).

⁶The absorption shoulder at 1.4 eV is absent in many samples of *trans*-polyacetylene prepared by the Durham synthesis route (see Ref. 5).

⁷E. J. Mele, *Synth. Met.* **9**, 207 (1984).

⁸J. Yu, H. Matsuoka, and W. P. Su, *Phys. Rev. B* **37**, 10367 (1988).

⁹G. B. Blanchet, C. R. Fincher, T. C. Chung, and A. J. Heeger, *Phys. Rev. Lett.* **51**, 2132 (1983).

¹⁰W. Franz, *Z. Naturforsch.* **13**, 484 (1958).

¹¹L. V. Keldysh, *Zh. Eksp. Teor. Fiz.* **34**, 1138 (1958) [*Sov. Phys.—JETP* **7**, 788 (1958)].

¹²A. Frova and P. Handler, in *Proceedings of the 7th International Conference on the Physics of Semiconductors, Paris*, edited by M. Hulin (Dunod, Paris, 1964), p. 157.

¹³A. Frova and P. Handler, *Appl. Phys. Lett.* **5**, 11 (1964).

¹⁴A. Frova and P. Handler, *Phys. Rev.* **37**, A1857 (1965).

¹⁵B. O. Seraphin, *Proceedings of the 7th International Conference on the Physics of Semiconductors, Paris*, edited by M. Hulin (Dunod, Paris, 1964), p. 165.

¹⁶B. O. Seraphin and N. Bottka, *Phys. Rev.* **139**, A560 (1965).

¹⁷B. O. Seraphin, R. B. Hess, and N. Bottka, *J. Appl. Phys.* **36**,

- 2242 (1965).
- ¹⁸D. E. Aspnes, in *Handbook on Semiconductors*, edited by T. S. Moss (North-Holland, Amsterdam, 1980), Vol. 1.
- ¹⁹M. Cardona, *Modulation Spectroscopy* (Academic, New York, 1969), Suppl. 11.
- ²⁰*Modulation Techniques, Semiconductors and Semimetals*, edited by R. K. Willardson and A. C. Beer (Academic, New York, 1972), Vol. 9.
- ²¹D. E. Aspnes and J. E. Rowe, *Solid State Commun.* **8**, 1145 (1970).
- ²²D. E. Aspnes and J. E. Rowe, *Phys. Rev. B* **5**, 4022 (1972).
- ²³D. E. Aspnes, *Surf. Sci.* **37**, 418 (1973).
- ²⁴F. Luty, *Surf. Sci.* **37**, 120 (1973).
- ²⁵U. M. Grassano, *Nuovo Cimento* **39**, 368 (1977).
- ²⁶J. D. Dow, in *Optical Properties of Solids*, edited by B. O. Serpahn (North-Holland, New York, 1976), Chap. 2.
- ²⁷D. A. B. Miller, D. S. Chemia, T. C. Damen, A. C. Gossard, W. Wiegmann, T. H. Wood, and C. A. Burrus, *Phys. Rev. B* **32**, 1043 (1985).
- ²⁸L. Sebastian, G. Weiser, and H. Bassler, *Chem. Phys.* **61**, 125 (1981).
- ²⁹L. Sebastian, G. Peter, and H. Bassler, *Chem. Phys.* **75**, 103 (1983).
- ³⁰L. Sebastian and G. Weiser, *Chem. Phys. Lett.* **64**, 396 (1979). PTS stands for polydiacetylene-2,4-hexadiyne-1,6-diol(*p*-toluenesulfonate).
- ³¹L. Sebastian and G. Weiser, *Phys. Rev. Lett.* **46**, 1156 (1981). DCHD stands for polydiacetylene-1,6-di(*N*-carbazolyl)-2,4-hexadiyne.
- ³²Y. Tokura, Y. Oowaki, T. Koda, and R. H. Baughman, *Chem. Phys.* **88**, 437 (1984). TCDU stands for polydiacetylene-5,7-dodecadiyne-1,12-diolbis(phenylurethane).
- ³³N. F. Colaneri, R. H. Friend, H. E. Schaffer, and A. J. Heeger, *Phys. Rev. B* **38**, 3960 (1988).
- ³⁴R. Worland, S. D. Phillips, W. C. Walker, and A. J. Heeger, *Synth. Met.* **28**, D663 (1989).
- ³⁵G. Leising, *Phys. Rev. B* **38**, 10313 (1988).
- ³⁶P. T. Townsend and R. H. Friend, *Synth. Met.* **17**, 403 (1987).
- ³⁷H. Shirakawa and S. Ikeda, *J. Polym. Sci. Polym. Chem. Ed.* **12**, 11 (1974).
- ³⁸K. Akagi, M. Suezaki, H. Shirakawa, H. Kyotani, M. Shimomura, and Y. Tanabe, *Synth. Met.* **28**, D1 (1989).
- ³⁹Dielectric screening can occur in any material of nonzero conductivity when the electrical contacts are not perfectly Ohmic.
- ⁴⁰M. Sinclair, D. Moses, R. H. Friend, and A. J. Heeger, *Phys. Rev. B* **36**, 4296 (1987).
- ⁴¹B. R. Weinberger, C. B. Roxio, S. Etemad, G. L. Baker, and J. Orenstein, *Phys. Rev. Lett.* **53**, 86 (1984).
- ⁴²The authors are grateful to Professor G. Leising for supplying the linear optical constants of oriented *trans*-polyacetylene.
- ⁴³A. Yariv, *Optical Electronics*, 3rd ed. (Holt, Rinehart, and Winston, 1985), Chap. 9.
- ⁴⁴H. Eckhardt, *J. Chem. Phys.* **79**, 2085 (1983).
- ⁴⁵D. Moses, A. Feldblum, E. Ehrenfreund, A. J. Heeger, T. C. Chung, and A. G. MacDiarmid, *Phys. Rev. B* **26**, 3361 (1982).
- ⁴⁶N. F. Mott and W. D. Tworse, *Adv. Phys.* **10**, 107 (1961).
- ⁴⁷E. Ehenfreund, Z. Vardeny, O. Brafman, and B. Horovitz, *Phys. Rev. B* **36**, 1535 (1987).
- ⁴⁸P. Vogl, D. K. Campbell, and O. F. Sankey, *Synth. Met.* **28**, D513 (1989).